JM PAPERS

Effects of fetch length on turbulent boundary layer recovery past a step change in surface roughness

Martina Formichetti[1] , **Dea D. Wangsawijaya**[1] , **Sean Symon**[1] and **Bharathram Ganapathisubramani**[1]

[1]Department of Aeronautical and Astronautical Engineering, University of Southampton, University Road, Southampton SO17 1BJ, UK

Corresponding author: Martina Formichetti, martina.formichetti@soton.ac.uk

Recent studies focusing on the response of turbulent boundary layers (TBLs) to a step change in roughness have provided insight into the scaling and characterisation of TBLs and the development of the internal layer. Although various step-change combinations have been investigated, ranging from smooth-to-rough to rough-to-smooth, the minimum required roughness fetch length over which the TBL returns to its homogeneously rough behaviour remains unclear. Moreover, the relationship between a finite- and infinite-fetch roughness function (and the equivalent sand-grain roughness) is also unknown. In this study, we determine the minimum 'equilibrium fetch length' for a TBL developing over a smooth-to-rough step change as well as the expected error in local skin friction if the fetch length is under this minimum threshold. An experimental study is carried out where the flow is initially developed over a smooth wall, and then a step change is introduced using patches of P24 sandpaper. Twelve roughness fetch lengths are tested in this study, systematically increasing from $L = 1\delta_2$ up to $L = 39\delta_2$ (where L is the roughness fetch length and δ_2 is the TBL thickness of the longest fetch case), measured over a range of Reynolds numbers ($4 \times 10^3 \leqslant Re_\tau \leqslant 2 \times 10^4$). Results show that the minimum fetch length needed to achieve full equilibrium recovery is around $20\delta_2$. Furthermore, we observe that the local friction coefficient, C_f, recovers to within 10 % of its recovered value for fetch lengths $\geqslant 10\delta_2$. This information allows us to incorporate the effects of roughness fetch length on the skin friction and roughness function.

Key words: turbulent boundary layers

M. Formichetti, D.D. Wangsawijaya, S. Symon and B. Ganapathisubramani

1. Introduction

Turbulent boundary layers (TBLs) developing over rough walls are found in many engineering applications. Studying this phenomenon is crucial for the performance evaluation of an engineering system. For example, in the aeronautical or automotive industry, the manipulation of a TBL using a surface treatment (i.e. roughness) may result in drag reduction (Whitmore & Naughton 2002). On the other hand, in the wind energy sector, an atmospheric boundary layer (ABL) in neutral conditions developing over a wind farm behaves like a large-scale TBL over roughness. Understanding the physics of this flow leads to more accurate wind power predictions and strategic site selections (Bou-Zeid *et al.* 2020).

A realistic representation of a rough-wall TBL in these applications hardly ever involves a homogeneous rough wall. In some scenarios, it can be better approximated with a streamwise transition in roughness. For example, the roughness on a ship hull (due to biofouling and coating deterioration) forms at various roughness length scales and sites, resulting in multiple streamwise transitions in roughness that affect the development of the TBL. At the same time, when analysing sites for wind farm locations we might encounter areas of complex terrain where we see a combination of forests and plains or sea and coastline. These variations significantly affect the behaviour of the ABL and, consequently, the drag production near the surface.

The main change occurring in a TBL over a rough wall compared with one over a smooth wall is an increase in wall shear stress (WSS). This results in a momentum deficit ΔU^+, characterised by a vertical shift in the logarithmic layer of the streamwise mean velocity profile, which, for fully rough flows, is defined as follows:

$$U^+ = \frac{1}{\kappa}\ln\left(y^+\right) + A - \Delta U^+ = \frac{1}{\kappa}\ln\left(\frac{y}{k_s}\right) + B, \tag{1.1}$$

where $\kappa \approx 0.39$, $A \approx 4.3$ and $B = 8.5$. Equation (1.1) shows that the two main parameters used to scale TBLs over rough walls are k_s as the length scale, and the friction velocity u_τ (see Jiménez (2004) or other similar works for the details on the scaling arguments). A surface with arbitrary representative roughness height k is associated with a length scale k_s, as shown in figure 1, which affects the logarithmic layer of the mean velocity profile in the same way as a surface covered by an ideally uniform sand-grain type of roughness with physical height k_s. Its definition is given in Colebrook *et al.* (1937) and Nikuradse (1933) and some examples of its usage can be found in Flack & Schultz (2014) and Schultz & Flack (2009). This height is usually calculated by taking a point measurement in the logarithmic layer of a TBL and using (1.1), with the main assumption being that the flow is within the fully rough regime. Another method of calculating k_s is given by Monty *et al.* (2016), which consists of an iterative procedure to obtain a direct relation between the surface friction and k_s. This method assumes that the TBL adheres to the outer layer similarity (see Townsend 1965). As such, the TBL is in equilibrium with the surface texture.

A TBL past a step change in roughness undergoes a well-documented change in its internal structure (Elliott 1958; Townsend 1965). Specifically, the logarithmic region of the TBL is split into two parts: an internal layer (IL), mostly in equilibrium with the downstream roughness, and an outer layer, still in equilibrium with the upstream surface. Whilst k_s has traditionally been defined as a constant, it can be argued that this assumption may overlook significant opportunities to account for deviations from idealised roughness effects. In fact, the mean velocity in the two log regions of the TBL past a step change in
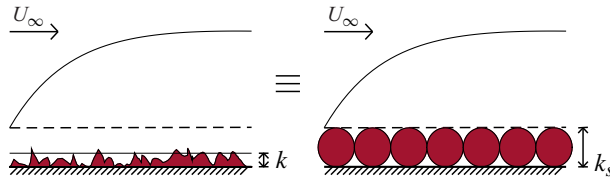
Figure 1. Schematic of physical roughness height k vs. the equivalent sand-grain roughness height k_s.

roughness can be described using (1.1) by allowing k_s to vary and reflect the surface with which the region is in equilibrium. Furthermore, varying k_s as a function of fetch length might provide a straightforward way to describe the onset of equilibrium in the IL and its development within the TBL until equilibrium is achieved throughout the entire structure. This will be discussed in more detail in § 3.

Another effect of step changes in roughness is the immediate impact on WSS and its recovery to an equilibrium state. This phenomenon has been extensively studied using both experimental and numerical approaches. The WSS either increases or decreases abruptly overshooting or undershooting the expected value for the downstream surface in smooth-to-rough (Bradley 1968; Antonia & Luxton 1971*a*) and rough-to-smooth transitions (Antonia & Luxton 1972; Efros & Krogstad 2011; Hanson & Ganapathisubramani 2016), respectively. Experimentally, this has been researched with direct WSS measurements immediately downstream of the step change by using floating element balances (Bradley 1968; Efros & Krogstad 2011), near-wall hot-wires (Chamorro & Porté-Angel 2009), Preston tubes (Loureiro *et al.* 2010) and pressure taps (Antonia & Luxton 1971*a*, 1972), coupled with indirect methods to obtain the development of the WSS with distance from the step change. This was mainly done using a logarithmic fit to match the measured value and the expected one for the downstream surface if there were no surface changes upstream. Numerically, the WSS recovery after a step change in roughness has been mainly investigated with direct numerical simulations (Lee 2015; Ismail *et al.* 2018*a*; Rouhi *et al.* 2019*b*) and large eddy simulations (Saito & Pullin 2014; Sridhar 2018). The results of all these studies were conducted at friction Reynolds numbers in the range $10^2 \leqslant Re_\tau \leqslant 10^6$, and a variety of downstream-to-upstream roughness height ratios, $-6 \leqslant \ln(k_{s,2}/k_{s,1}) \leqslant 6$ (where the subscripts 1 and 2 indicate the values for the upstream and downstream surfaces, respectively). Here, negative ratios correspond to rough-to-smooth transitions, and positive values correspond to smooth-to-rough changes.

Previous studies highlighted some remaining questions regarding the TBL recovery to an equilibrium condition after being subjected to a streamwise step change in roughness. Firstly, as mentioned above, the characteristic overshoot or undershoot of the WSS just after a step change in roughness renders the characterisation methods developed for the homogeneous rough wall inaccurate, since both scaling parameters depend on WSS and are calculated assuming fully rough homogeneous roughness. This leads to a need to define a minimum recovery length in which the flow recovers to the homogeneous rough-wall TBL. Secondly, the use of experimental indirect methods and numerical methods to obtain the WSS recovery after a step change resulted in a wide range of recovery fetch lengths between 1δ and 10δ, making it difficult to draw specific conclusions from these predictions. Moreover, some studies such as Saito & Pullin (2014) and Sridhar (2018) showed an increase in recovery fetch length with Reynolds number which is inconsistent with other studies, highlighting the necessity of a direct WSS measurement method for a more accurate prediction. An extensive review and comparison between existing studies can be found in Li *et al.* (2019).
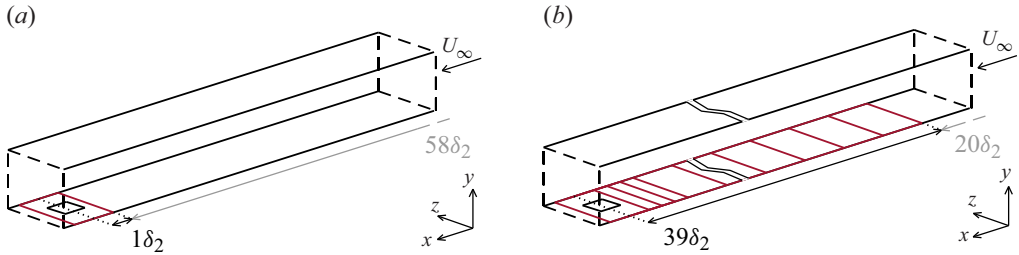
Figure 2. Schematic of the experiment with the fetch length, L, measured from the centreline of the balance: (*a*) $L = 1\delta_2$ and (*b*) $L = 39\delta_2$.

In this study, we consider a TBL developing from a baseline smooth wall and subjected to a streamwise transition to a rough wall. We aim to investigate and achieve a reliable value for the minimum roughness fetch length that allows a TBL developing past such step change in roughness to recover to an equilibrium condition, i.e. fully adjust to the rough wall downstream of the transition. This is essential since all of the scaling arguments used in rough-wall TBLs depend on the WSS and the latter changes drastically after a step change in wall roughness. Secondly, we aim to quantify the error in choosing a shorter fetch to conduct experiments/simulations on presumably homogeneous fully rough flows. This would be helpful to quantify the uncertainty of the data if, for instance, a study needed to be conducted in a facility with a shorter test section, or if there were limitations on the domain size for a numerical investigation dictated by the available computational power. Finally, we aim to develop a relationship between the k_s value of a surface with short fetch (where the flow is not in equilibrium) in terms of the equilibrium value of k_s. We designed an experiment to directly measure the change in WSS to sequential increases in roughness fetch, covering a wide range of Reynolds numbers, $4 \times 10^3 \leqslant Re_\tau \leqslant 2 \times 10^4$, to ensure all or most common conditions are covered. The set-up of the experiment is covered in § 2, followed by a detailed discussion of the results in § 3 leading to the conclusions and future work in § 4.

2. Experimental set-up and methodology

The experimental campaign is conducted inside the closed return boundary layer wind tunnel (BLWT) at the University of Southampton. The TBL is tripped by a turbulator tape located at the inlet of the test section, marking the streamwise datum ($x = 0$) and further developed along the floor of the 12 m-long test section, which has a width and height of 1.2 m and 1 m, respectively. Figure 2 illustrates the tunnel and coordinate system where x, y and z denote the streamwise, wall-normal and spanwise directions, respectively. The tunnel is equipped with a 'cooling unit' comprising two heat exchangers and a temperature controller such that the air temperature remains constant during measurements (21°C ±0.5°C). The free stream has a turbulence intensity of less than 0.1 % of the free-stream velocity U_∞, which is measured with hot-wire anemometry before the experimental campaign. The tunnel is equipped with a closed-loop feedback controller to set U_∞, and air properties are measured with a Pitot-static tube and a thermistor inside the BLWT.

As seen in figure 2, the experiment consisted of a roll of P24 sandpaper cut in patches of size $2\delta_2 \times 8\delta_2$, where δ_2 refers to the TBL thickness of the case with the longest fetch measured at the balance location. This length scale was chosen instead of the more commonly used δ_1 (where δ_1 is the TBL thickness over the smooth surface measured at the measurement point) for two reasons. Firstly, having the recovery length as a function
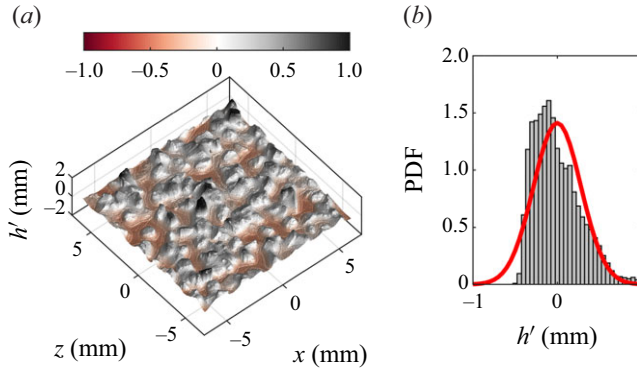
Figure 3. Laser scan of the P24 sandpaper used in the campaign with probability density function (PDF) of the surface height variation, h' from the mean physical height $\overline{h}$. Key surface statistics are as follows: $k = 6\sqrt{\overline{h'^2}} = 1.6953$, $k_a = \overline{|h'|} = 0.2257$, $k_p = \max(h') - \min(h') = 2.0227$, $k_{rms} = \sqrt{\overline{h'^2}} = 0.2825$.

of the downstream TBL thickness removes all dependency on the type of surface upstream of the step change, making it applicable to more cases. Secondly, the TBL thickness was measured using particle image velocimetry (PIV) above the balance to ensure consistency between the balance readings and the flow field above while no PIV measurement was taken upstream of the step change in any of the cases. For the sake of clarity, the relationship between δ_1 and δ_2 in the current experimental campaign is quantified. This analysis is based on PIV measurements of the smooth wall at the measurement location, combined with the equation for the evolution of δ over a smooth surface ($\delta = 0.37x/Re_x^{1/5}$, White 2011) to estimate the value at the step-change location for the case where the TBL achieves equilibrium. The resulting ratio, $\delta_1/\delta_2 \approx 0.8$, provides a basis for direct comparison with previous studies.

The patches are sequentially taped on the floor of the wind tunnel's test section starting at the measurement point, which is located approximately $59\delta_2$ downstream from the test section's inlet. The patches are then added upstream, so that the roughness fetch measured from the centreline of the balance is systematically increased. The shortest fetch is $1\delta_2$, and the longest is $39\delta_2$, which corresponds to the distance between the measurement point and the step change in roughness. This means that, for the longest fetch configuration, the distance between the step change in roughness and the test section inlet is approximately $20\delta_2$, while the distance between the measurement point and the step change in roughness is approximately $39\delta_2$, as shown in figure 2. A laser scan of the sandpaper used in the experimental campaign can be found in figure 3. The mean physical height, k of the sandpaper was computed as $k = 6\sqrt{\overline{h'^2}}$, similarly to Gul & Ganapathisubramani (2021), with h' being the variation from the mean surface height showed in figure 3 and $\sqrt{\overline{h'^2}}$ being the surface variance.

All cases tested in the experimental campaign are listed in table 1. The longest fetch tested was chosen as a threshold between having as long of a roughness fetch as achievable in our facility and ensuring the TBL on the smooth surface upstream of the step change would also have enough development length to be in equilibrium conditions ($\approx 25\delta_1$ or $\approx 20\delta_2$). As the sandpaper sheets are taped on the smooth wall, there is a step change of physical height k at the smooth-to-rough transition. The effect of the physical height difference between the smooth wall and the sandpaper taped onto it has been previously explored in Antonia & Luxton (1971a,b). Both experiments yielded the same results in

$1\delta_2$	$1.6\delta_2$	$2.2\delta_2$	$3\delta_2$	$5\delta_2$	$7\delta_2$	$9\delta_2$	$11\delta_2$	$15\delta_2$	$19\delta_2$	$27\delta_2$	$39\delta_2$
▼	▼	▼	▼	▼	▽	▽	▽	▽	▽	▽	▽

Table 1. Colour legend for different roughness fetches applied to all plots in § 3.

terms of $\overline{u'v'}$ distribution and WSS. Therefore, the physical height difference plays a negligible role on the flow development. Thus, we did not implement a system to isolate the effects of the superposition of the physical height of the two surfaces from the step change in roughness.

The experimental campaign was designed to take direct WSS measurements at different Reynolds numbers and with sequentially increased roughness fetch (the distance between the step change in roughness and the measurement point). This was possible by employing a floating element drag balance (located at the previously mentioned measurement point), designed and manufactured by Ferreira *et al.* (2024). With this tool, the friction on the wall was monitored during velocity sweeps (0–40 ms^{-1}) while systematically increasing the length of the roughness fetch. The velocity sweeps were run three times per case to ensure the repeatability of the results. The measurement uncertainty of skin friction from the balance is estimated to be less than 1 %. A detailed description of the balance, its specifications as well as uncertainty quantification can be found in Ferreira *et al.* (2024).

For each fetch length, measurements are conducted within a range of free-stream velocities $10\ \mathrm{ms}^{-1} \leqslant U_\infty \leqslant 40\ \mathrm{ms}^{-1}$, allowing 10 s for the flow to adjust after each velocity increase and 60 s for the flow to come to rest completely before restarting the sweep. The sampling rate was set to $f_s = 256$ Hz, while the sampling time was set to 60 s. Once the friction force, F, has been measured, the WSS, τ_w, and friction velocity, u_τ, can be directly computed

$$\tau_w = \frac{F}{A} = \frac{1}{2}\rho U_\infty^2 C_f = \rho u_\tau^2, \tag{2.1}$$

where A is the surface area of the balance plate and C_f is the friction coefficient.

Planar PIV was also performed in the streamwise wall-normal plane above the floating element location. This was done to check whether the outer layer similarity (OLS) used in Monty *et al.* (2016) to calculate k_s holds for some or all of our cases and to calculate the boundary layer thickness for all cases. The additional PIV measurements were only conducted at a free-stream velocity of 20 ms^{-1} and only for the cases with fetch length $1\delta_2$, $3\delta_2$, $5\delta_2$, $7\delta_2$, $9\delta_2$, $19\delta_2$ and $39\delta_2$. The selection of free-stream velocity and fetches to study with PIV was dictated by the trends obtained in the drag balance measurements, as seen in § 3. The data were sampled at $f_s = 1$ Hz ($t_r = N \times U_\infty/(f_s \times \delta_2) \approx 267 \times 10^3$, where t_r is the TBL turnover rate, $U_\infty = 20$ ms^{-1} and N is the number of samples taken, Marusic *et al.* (2015)) with Lavision Imager CMOS 25 MP cameras (resolution of 17 pixels mm^{-1}), using a Bernoulli 200 mJ, 532 nm Nd:YAG laser and the Lavision software Davis 10 for acquisition. The data were processed using an in-house code for cross-correlation, with a final window size of 16×16 px with 75 % overlap, and a viscous-scaled final window size $\Delta x^+ \times \Delta y^+$ of 30×30. The uncertainty in the mean flow is approximately 2 %, estimated following standard uncertainty propagation methods Bendat & Piersol (2010).
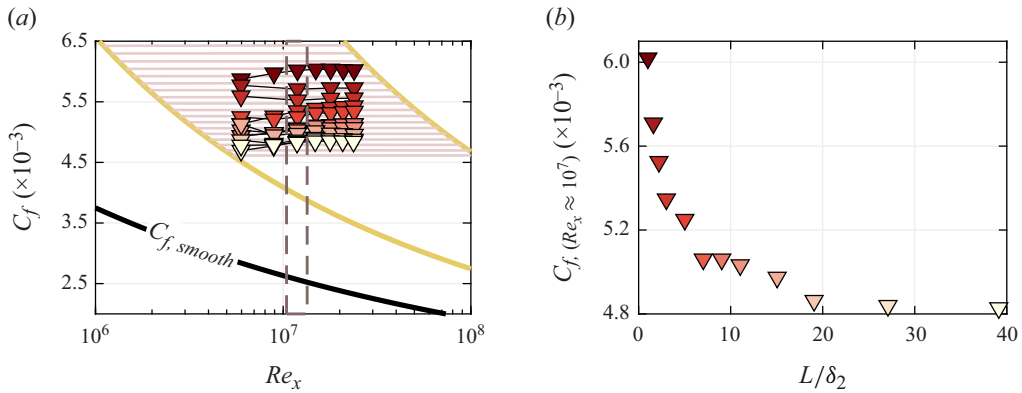
1009 A66-6

Figure 4. Panel (*a*) shows C_f plotted against $Re_x = U_\infty x/\nu$, where x is the distance of the balance centreline from the test section's inlet, with (——3) being lines of constant unit $Re = U_\infty/\nu$ (while fetch length x varies), and (——4) lines of constant k_s/x (while unit Re varies) as described by Monty *et al.* (2016). Panel (*b*) shows C_f at $Re_x \approx 10^7$ plotted against the fetch length L normalised by the downstream TBL thickness δ_2.

L [m]	$1\delta_2$	$3\delta_2$	$5\delta_2$	$7\delta_2$	$9\delta_2$	$19\delta_2$	$39\delta_2$
δ_{99} [m]	0.1202	0.1205	0.1219	0.1262	0.1265	0.1292	0.1495

Table 2. The TBL thickness at the drag balance location of the cases tested with PIV, fetch length defined as a function of δ_2 (the TBL thickness of the case with longest fetch).

3. Results

The colour legend for all the plots in § 3 is shown in table 1.

The evolution of the friction coefficient obtained with the drag balance at different fetch lengths and increasing Reynolds number ($Re_x = \rho U_\infty x/\mu$, where x is the streamwise distance between the wind tunnel's test section inlet and the balance centreline) can be seen in figure 4(*a*). This plot shows that, for a fixed fetch length, C_f is independent of Re_x, which is a sign that the flow is within the fully rough regime bounds mentioned in § 1. However, it is not fetch-length independent since the fetch length is inversely proportional to C_f, consistent with the overshoot downstream of the transition observed by multiple studies listed in Li *et al.* (2019), and the slow recovery with increasing distance from the step change.

The recovery of WSS with fetch length is shown more clearly in figure 4(*b*). This plot shows the recovery of the friction coefficient measured at around 20 ms^{-1} with fetch length. This is the lowest flow speed at which the TBL seems to reach fully rough conditions and is thus used for the PIV measurements as well. The friction coefficient is plotted against the normalised fetch length, where δ_2 is the boundary layer thickness at the balance location of the fully rough case with a fetch length of $\approx 39\delta_2$. For clarity, table 2 lists the TBL thickness measured above the balance for all the different fetches.

Figure 1(*b*) in Li *et al.* (2019) presents a comparison of recovery lengths compiled from previous studies, indicating a wide range of recovery lengths, from 1 to 10 δ_1, for both smooth-to-rough and rough-to-smooth transitions. The criteria for defining convergence in these studies remain unclear, with Li *et al.* (2019) suggesting, as an example, defining the recovery length L as the downstream fetch where the local C_f reaches approximately 80 % of the full-recovery value C_{f0}. Applying this criterion to our data (shown in figure 4*b*)
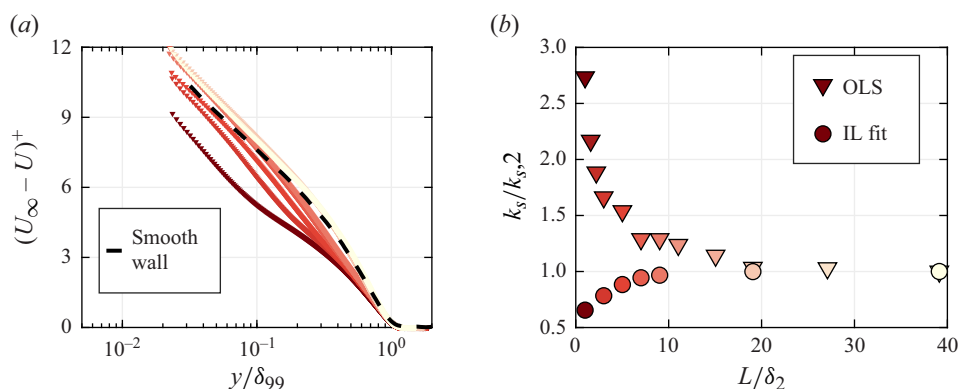
Figure 5. Panel (*a*) shows velocity defect plotted against y normalised by δ_{99} as listed in table 2 for each case. Panel (*b*) shows k_s evolution, normalised by $k_{s,2}$, with fetch length L scaled with δ_2. $k_{s,IL}$ and $k_{s,OLS}$ calculated at https://www.cambridge.org/S0022112025003118/files/figure5B.

suggests a recovery length of approximately $6\delta_2$, where C_f reaches 80 % of the equilibrium value. However, we propose an alternative criterion for convergence, defining it as the fetch where C_f plateaus within 5 % of the full-recovery value. Using this definition, our results indicate a longer recovery length of at least $20\delta_2$. Secondly, although we expect the overshoot in C_f immediately after transition (i.e. C_f measured in shorter patch lengths, $1\delta_2 - 5\delta_2$), we observe that, for $L > 10\delta_2$, the error in C_f is within ≈ 10 % of the converged value. This type of error is to be expected when a shorter development length or computational domain is used. Figure 4(*a*) can also be used to obtain the equivalent sand-grain height following the method proposed by Monty *et al.* (2016). As briefly mentioned in § 1, this method assumes that the flow has already reached an equilibrium state and therefore employs OLS from Townsend (1965), to obtain a relationship between C_f at constant unit Reynolds number and k_s, via what the authors refer to as lines of constant length, k_s/x. These are shown in figure 4(*a*) as pink horizontal solid lines. The intersection of these and the C_f values at given Re_x, give us a way of calculating k_s for different fetch lengths.

Before discussing the result of this operation, the OLS hypothesis from Townsend (1965) was reproduced and is shown in figure 5(*a*). From this plot, it can be seen that, for shorter fetch lengths, velocity defect profiles do not collapse and hence do not conform to OLS. This is to be expected as OLS is a measure of equilibrium with the boundary layer and for fetches lower than $\approx 10\delta_2$ equilibrium cannot be achieved due to the development of the IL. On the other hand, for the longer fetches, OLS can be observed as the profiles perfectly collapse onto smooth-wall TBLs from $\approx 0.4\delta$. The latter is the main conclusion from Townsend (1965), which means that the near-wall region and anything that is associated with it should not affect the outer portion of the TBL. From our results, we can conclude that this indeed holds for the longest fetches tested. In the following analysis, we will see more in detail how the non-equilibrium conditions affect the prediction of k_s values based on OLS and how this compares with the standard practice of calculating it from the roughness function ΔU^+ where fully rough as well as equilibrium conditions are assumed.

In figure 5(*b*) we show the k_s development with fetch length obtained using two methods. Firstly, the method from Monty *et al.* (2016) defined by the symbol ▼5; secondly, we used an IL curve fitting method to obtain k_s. In order to only fit the IL region, we used the first derivative of the Reynolds shear stress, which will be discussed later on in

1009 A66-8

figure 7, with respect to the natural log of y/δ_2. This highlighted a region of blending between two distinct profiles that we identified as the IL thickness. Finally, below this point we used (1.1) to curve fit the data. This is represented by the symbol ●6. Starting with the method from Monty *et al.* (2016) we observe that k_s follows the same trend as C_f, i.e. overshooting its 'real' value for a certain surface at fixed Reynolds number and logarithmically approaching its true value with increasing fetch length. Figure 5(*b*) shows how crucial it is to ensure sufficient fetch length for the WSS to recover to be able to treat k_s as universal and use it as a length scale/modelling constant for rough-wall TBLs. It can also be noted that the minimum fetch length for full WSS recovery is around $L \geqslant 20\delta_2$, where C_f becomes both Reynolds number and fetch-length independent. We note here that this streamwise fetch might depend on the type of roughness and the extent of change in k_s (from upstream to downstream). Regardless, the results suggest that TBLs flowing over a change in wall texture with fetch lengths shorter than at least $10\delta_2$ (error $\geqslant 10\%$) will inevitably result in a significant overestimation of the roughness function and corresponding mean flow.

In figure 5(*b*), we also see the trend of k_s when calculated by fitting a logarithmic profile to the velocity profile in the near-wall region (i.e. below the inflection point), which is the point where the IL blends into the outer layer. As shown in this figure, the trend captured by this method is opposite to the one given by the method in Monty *et al.* (2016) used previously. Nonetheless, the fetch length at which we can infer equilibrium conditions after a step change does not change and is in full agreement between the two methods. Moreover, the converged value of k_s for the longer fetch cases appears to be in perfect agreement as well. The challenge in using this method lies in accessing velocity measurements in the region close to the wall with enough resolution to fit a logarithmic profile and achieving a Reynolds number large enough to be able to distinguish the inflection point.

In this article, we propose using the equivalent sand-grain roughness height, k_s, as a parameter to describe and model TBLs over streamwise variations in surface roughness. This approach is motivated by the challenges associated with using the IL growth rate, which is highly dependent on the criteria used to identify the inflection point where the log region governed by the downstream roughness meets that in equilibrium with the upstream surface. As highlighted in the literature (e.g. Antonia & Luxton 1971*a*,*b*, 1972), the same case can often be interpreted with markedly different power laws depending on the chosen criteria, making it difficult to draw generic conclusions. In contrast, k_s offers a simpler and more consistent parameter for characterising the effects of step changes in surface roughness.

We propose redefining k_s as a function of fetch length with the form

$$\lim_{x \to \infty} k_s(x) = k_{s,}\text{homogeneous.} \tag{3.1}$$

This approach aligns with the physical processes governing the development of equilibrium and is consistent with existing wall models for low-fidelity simulations. In Reynolds-averaged Navier–Stokes models, roughness is typically applied using the law of the wall with k_s specified *a priori*. By allowing k_s to vary with fetch length, this approach improves the reliability of low-fidelity simulations in TBL studies while maintaining computational efficiency and simplicity.

Figure 6 shows the streamwise-averaged mean flow profiles measured by PIV, taken above the drag balance and scaled by the friction velocity given by the balance measurement, where the black dashed line represents the log profile. In figure 6(*a*), the wall-normal coordinate used to plot all the profiles is normalised by the fully rough, equilibrium value of $k_s = k_{s,2}$, which is computed for the longest fetch case. Here, we
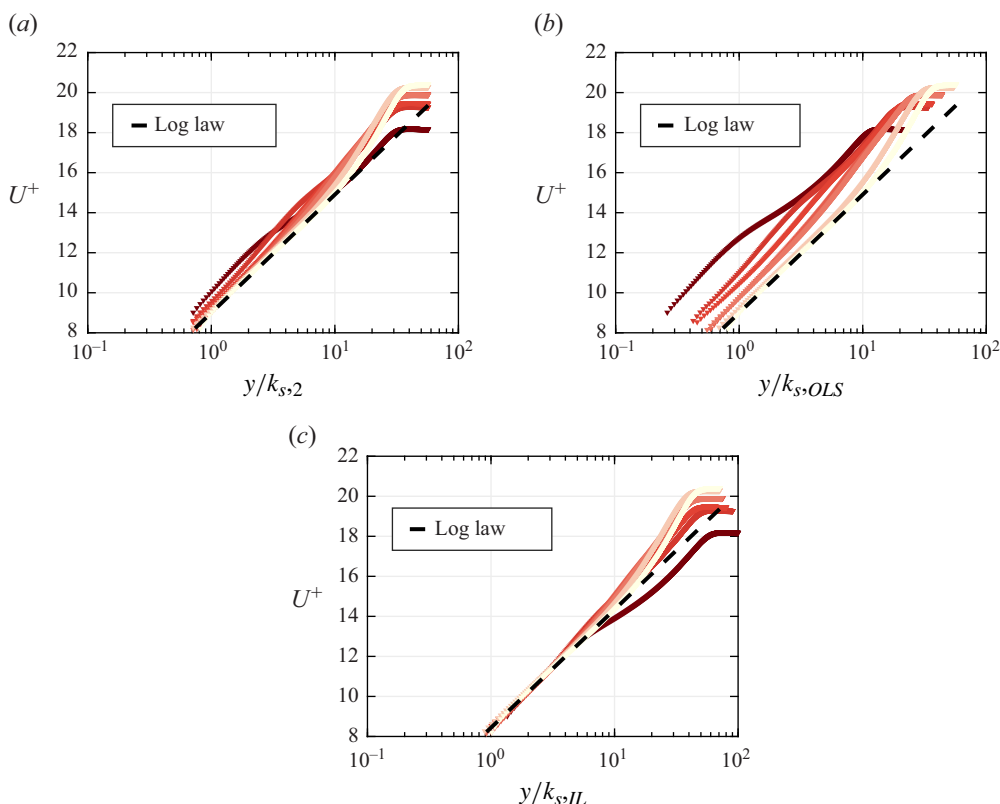
(*a*)

(*b*)

(*c*)

Figure 6. Velocity in viscous units plotted against the wall-normal coordinate normalised by (*a*) $k_{s,2}$ given by the longest fetch case, (*b*) $k_{s,OLS}$ shown with the symbol ▼7 in figure 5(*b*) and (*c*) $k_{s,IL}$ shown with the symbol ●8 in figure 5(*b*).

can see that, although the two longest fetches collapse onto the dashed line perfectly in the log region, the rest of the cases slowly diverge from it with the shortest fetch displaying a change in slope across the logarithmic domain of the TBL. This is clearly explained by the blending of the logarithmic regions from the upstream and downstream surface near the step change in roughness. In the next plot, figure 6(*b*), we used a k_s value for each fetch case that attempts to include the effect of the IL development by computing it using the local C_f value as described in Monty *et al.* (2016) and shown in figure 5(*b*) – 'OLS'. However, when using this method, the profiles seem to diverge to a greater extent than using the $k_{s,2}$ value for all the cases. This can be explained by the equilibrium assumption made when employing the method described in Monty *et al.* (2016). Lastly, in figure 6(*c*), we used the k_s value for each individual case given by fitting a logarithmic profile to the IL only as shown in figure 5(*b*) – 'IL fit'. Using this method we achieved a perfect match for all fetches below the inflection point, while above this point the shorter fetch profiles do not collapse onto the longer ones. This is because the k_s value that models the IL region would inevitably fail in the outer region in cases of non-equilibrium such as a TBL after a step change in roughness. Therefore, in order to achieve a universal scaling we would have to make k_s a function of x, by employing a different value for different fetches, and y, by using a different value below and above the inflection points where the IL is still developing. Finally, this method is only possible when a direct way of measuring drag is available as the drag given by the slope of the IL is not correct for short fetches.
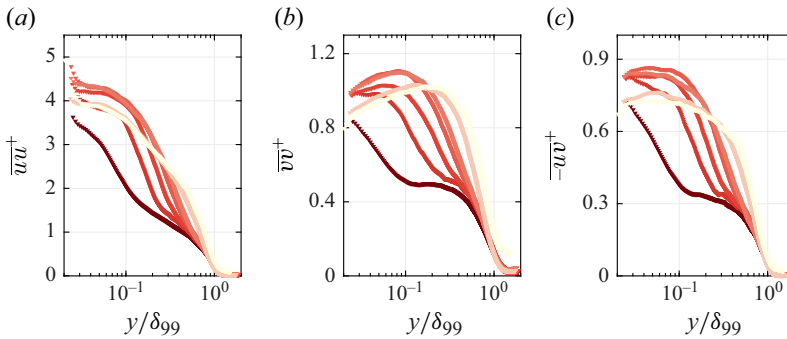
Figure 7. Turbulent fluxes (*a,b*), and Reynolds shear stress (*c*), in viscous units against wall-normal distance in outer scaling.

Finally, we looked at the second-order statistics for all cases and compared the patterns with the mean fields that we discussed above. Figure 7 illustrates the turbulent intensities (panels a and b) and Reynolds shear stress (panel c) in viscous units, plotted against the wall-normal distance using outer scaling. These plots allow for a detailed examination of the onset and development of equilibrium within the TBL downstream of the step change in roughness.

From these profiles, it is evident that equilibrium is achieved at approximately $20\delta_2$, as the curves align closely with those of the longest fetch case. This observation aligns with the mean velocity analysis presented in figure 6. Additionally, the growth of the IL within the TBL is particularly pronounced in all the second-order statistics plots, especially for the shortest fetches of $1\delta_2$ and $3\delta_2$. For these cases, a noticeable change in the curvature of the turbulent profiles is apparent, with the transition occurring closer to the wall for the shortest fetch and gradually extending outward with increasing fetch length.

4. Conclusions

The current paper aims to describe the outcome of an experimental campaign involving direct measurements of the WSS recovery after a step change in wall roughness with systematically increasing fetch length. The results show that full WSS recovery is achieved $20\delta_2$ downstream of the step change, while previous studies employing indirect ways of measuring the WSS recovery predicted a full recovery between $1\delta_1$ and $10\delta_1$. This difference is most likely due to the logarithmic nature of the WSS recovery. Therefore, even the smallest difference in WSS results in a significant difference in fetch length. We also show that the greatest change in WSS appears for fetch lengths between $1\delta_2$ and $10\delta_2$, resulting in an error of $\leqslant 10\,\%$ of the converged WSS value when fetches $\geqslant 10\delta_2$ are used.

Moreover, we have shown that the equivalent sand-grain height, k_s, given by the method adopted in Monty *et al.* (2016) cannot be used to scale or model the mean velocity profile of a TBL for fetches measuring less than $10\delta_2$, as this would inevitably result in a significant overprediction of the roughness effects and erroneous velocity profiles. This is due to the assumptions employed when deriving k_s, including fully rough regime and equilibrium conditions in the TBL, which do not apply in the case of a TBL flowing past a step change with fetch length measuring less than $10\delta_2$. On the other hand, when fitting a logarithmic profile to the IL region, we can achieve a unique k_s value for finite fetches that is able to scale/model the velocity profile below the inflection point and, by making k_s vary in the wall-normal direction, we could be able to model TBLs past step changes in roughness and their development to a greater extent.

A new way of modelling k_s, which takes into account both log regions of the internal boundary layer downstream of the transition and the outer layer (containing the flow history prior to the transition), could help with modelling streamwise-varying rough-wall TBLs. A correction factor between the k_s trend with increasing fetch given by Monty *et al.* (2016) and the one given by fitting should also be developed in cases where high-resolution PIV at the right Reynolds number near the wall is not viable.

REFERENCES

ANTONIA, R.A. & LUXTON, R.E. 1971*a* The response of a turbulent boundary layer to a step change in surface roughness Part 1. Smooth to rough. *J. Fluid Mech.* **48** (4), 721–761.

ANTONIA, R.A. & LUXTON, R.E. 1971*b* The response of a turbulent boundary layer to an upstanding step change in surface roughness. *J. Basic Engng* **93** (1), 22–32.

ANTONIA, R.A. & LUXTON, R.E. 1972 The response of a turbulent boundary layer to a step change in surface roughness. Part 2. Rough-to-smooth. *J. Fluid Mech.* **53** (4), 737–757.

BENDAT, J.S. & PIERSOL, A.G. 2010 *Random Data, Anaysis and Measurement Procedures*. John Wiley and Sons.

BOU-ZEID, E., ANDERSON, W., KATUL, G.G. & MAHRT, L. 2020 The persistent challenge of surface heterogeneity in boundary-layer meteorology: a review. *Boundary-Layer Meteorol.* **177** (2–3), 227–245.

BRADLEY, E.F. 1968 A micrometeorological study of velocity profiles and surface drag in the region modified by a change in surface roughness. *Q. J. R. Meteorol. Soc.* **94** (401), 361–379.

CHAMORRO, L.P. & PORTÉ-ANGEL, F. 2009 Velocity and surface shear stress distributions behind a rough-to-smooth surface transition: a simple new model. *Boundary-Layer Meteorol.* **130** (1), 29–41.

COLEBROOK, C.F., WHITE, C.M. & TAYLOR, G.I. 1937 Experiments with fluid friction in roughened pipes. *Proc. R. Soc. Lond. A* **161** (906), 367–381.

EFROS, V. & KROGSTAD, P. 2011 Development of a turbulent boundary layer after a step from smooth to rough surfaces. *Exp. Fluids* **51** (6), 1563–1575.

ELLIOTT, W.P. 1958 The growth of the atmospheric internal boundary layer. *EOS Trans. AGU* **39** (6), 1048–1054.

FERREIRA, M.A., COSTA, P. & GANAPATHISUBRAMANI, B. 2024 Wall shear stress measurement using a zero-displacement floating-element balance. *Exp. Fluids* **65** (56).

FLACK, K.A. & SCHULTZ, M.P. 2014 Roughness effects on wall-bounded turbulent flows. *Phys. Fluids* **26** (10), 101305.

GUL, M. & GANAPATHISUBRAMANI, B. 2021 Revisiting rough-wall turbulent boundary layers over sand-grain roughness. *J. Fluid Mech.* **911**.

HANSON, R.E. & GANAPATHISUBRAMANI, B. 2016 Development of turbulent boundary layers past a step change in wall roughness. *J. Fluid Mech.* **795**, 494–523.

ISMAIL, U., ZAKI, T.A. & DURBIN, P.A. 2018*a* The effect of cube-roughened walls on the response of rough-to-smooth (RTS) turbulent channel flows. *Intl J. Heat Mass Transfer* **72**, 174–185.

JIMÉNEZ, J. 2004 Turbulent flows over rough walls. *Annu. Rev. Fluid Mech.* **36** (1), 173–196.

LEE, J.H. 2015 Turbulent boundary layer flow with a step change from smooth to rough surface. *Intl J. Heat Fluid Flow* **54**, 39–54.

LI, M., DE SILVA, C.M., CHUNG, D., PULLIN, D.I., MARUSIC, I. & HUTCHINS, N. 2019 Modelling the downstream development of a turbulent boundary layer following a step change of roughness. *J. Fluid Mech.* **949**, A7.

LOUREIRO, J.B.R., SOUSA, F.B.C.C., ZOTIN, J.L.Z. & FREIRE, A.P.S. 2010 The distribution of wall shear stress downstream of a change in roughness. *Intl J. Heat Mass Transfer* **31** (5), 785–793.

MARUSIC, I., CHAUHAN, K.A., KULANDAIVELU, V. & HUTCHINS, N. 2015 Evolution of zero-pressure-gradient boundary layers from different tripping conditions. *J. Fluid Mech.* **783**, 379–411.

MONTY, J.P., DOGAN, E., HANSON, R., SCARDINO, A.J., GANAPATHISUBRAMANI, B. & HUTCHINS, N. 2016 An assessment of the ship drag penalty arising from light calcareous tubeworm fouling. *Biofouling* **32** (4), 451–464.

NIKURADSE, J. 1933 *Laws of Flows in rough Pipes*. NACA.

ROUHI, A., CHUNG, D. & HUTCHINS, N. 2019*b* Direct numerical simulation of open-channel flow over smooth-to-rough and rough-to-smooth step changes. *J. Fluid Mech.* **866**, 450–486.

SAITO, N. & PULLIN, D.I. 2014 Large eddy simulation of smooth–rough–smooth transitions in turbulent channel flows. *Intl J. Heat Mass Transfer* **78**, 707–720.

SCHULTZ, M.P. & FLACK, L.A. 2009 Turbulent boundary layers on a systematically varied rough wall. *Phys. Fluids* **21** (1), 015104.

SRIDHAR, A. 2018 Large-eddy simulation of turbulent boundary layers with spatially varying roughness. PhD thesis, California Institute of Technology, USA.

TOWNSEND, A.A. 1965 The response of a turbulent boundary layer to abrupt changes in surface conditions. *J. Fluid Mech.* **22** (4), 799–822.

WHITE, F.M. 2011 *Viscous Fluid Flow*. 3rd edn. McFraw Hill Education.

WHITMORE, S.A. & NAUGHTON, J.W. 2002 Drag reduction on blunt-based vehicles using forebody surface roughness. *J. Spacecr. Rockets* **39** (4), 596–604.